



## Analysis of liquid–vapor pulsating flow in a U-shaped miniature tube

Yuwen Zhang<sup>a,\*</sup>, A. Faghri<sup>b</sup>, M.B. Shafii<sup>b</sup>

<sup>a</sup> Department of Mechanical Engineering, New Mexico State University, Las Cruces, NM 88001, USA

<sup>b</sup> Department of Mechanical Engineering, University of Connecticut, Storrs, CT 06269, USA

Received 23 July 2001; received in revised form 3 November 2001

### Abstract

Liquid–vapor pulsating flow in a vertically placed U-shaped miniature tube is investigated numerically. The two sealed ends of the U-shaped tube are the evaporator sections and the condenser section is located in the middle of the tube. The governing equations, obtained by analyzing the conservation of mass, momentum, and energy of the liquid and vapor plugs, are nondimensionalized and the pulsating flow is described by five nondimensional parameters. The numerical solution is obtained by employing an implicit scheme. The effects of various nondimensional parameters on the performance of the pulsating heat pipe were investigated. The empirical correlations of the amplitude and circular frequency of oscillation were also obtained. © 2002 Elsevier Science Ltd. All rights reserved.

### 1. Introduction

The pulsating liquid–vapor flow in a miniature tube can find its application in pulsating heat pipes (PHPs), which is a very effective heat transfer device that can be utilized to transfer large amount of heat [1]. The inner diameter of the PHPs must be sufficiently small so that the vapor plugs can be formed in the tube by growth of the vapor bubbles. The unique feature of PHPs is that there is no wick structure to return the condensate to the evaporator section, and therefore there is no counter current flow between the liquid and vapor. Applications of pulsating heat pipes are found in a wide range of practical problems including electronics cooling [2,3].

Miyazaki and Akachi [4] presented experimental investigation of heat transfer characteristics of a looped capillary heat pipe and found that heat transfer limitations that usually exist in the traditional heat pipes are not encountered in the PHP. The test results suggested that pressure oscillation and the oscillatory flow excite each other. A simple analytical model of self-excited oscillation was proposed based on such oscillating fea-

tures. Miyazaki and Akachi [6] derived the wave equation for pressure oscillation in an oscillating heat pipe based on self-excited oscillation, in which the reciprocal excitation between the pressure oscillation and void fraction is assumed. A closed form solution of wave propagation velocity was obtained by solving the wave equation. Miyazaki and Arikawa [5] presented experimental results on the oscillatory flow in the oscillating heat pipe and the measured wave velocity fairly agreed with the prediction of Miyazaki and Akachi [6].

Lee et al. [7] reported that the oscillation of bubbles is caused by nucleate boiling and vapor oscillation, and departure of small bubbles is considered as the representative flow pattern at the evaporator and adiabatic sections, respectively. Hosoda et al. [8] investigated propagation phenomena of vapor plugs in a meandering closed loop heat transport device. They observed a simple flow pattern appearing at high liquid volume fractions. At such a condition, only two vapor plugs exist separately in adjacent turns, and one of them starts to shrink when the other starts to grow. A simplified numerical solution was also performed with several major assumptions including neglecting liquid film which may exist between the tube wall and a vapor plug. Thermal modeling of vertically placed unlooped and looped PHP with three heating sections and two cooling sections was presented by Shafii et al. [9]. The dimensional governing

\* Corresponding author. Tel.: +1-505-646-6546; fax: +1-505-646-6111.

E-mail address: yuwzhang@nmsu.edu (Y. Zhang).

Nomenclature		Greek symbols	
$A$	dimensionless amplitude of pressure oscillation	$\gamma$	ratio of specific heat
$A_c$	cross-sectional area of the tube, $m^2$	$\theta$	dimensionless temperature
$B$	dimensionless amplitude of displacement	$\Theta$	dimensionless temperature difference
$C$	integration constant	$\nu_e$	effective viscosity, $m^2/s$
$c_p$	specific heat at constant pressure, $J/kg\ K$	$\rho$	density, $kg/m^3$
$c_v$	specific heat at constant volume, $J/kg\ K$	$\tau$	dimensionless time
$d$	diameter of the heat pipe, $m$	$\tau_p$	shear stress, $N/m^2$
$h$	heat transfer coefficient, $W/m^2\ K$	$\omega$	dimensionless angular frequency
$H$	dimensionless heat transfer coefficient	$\omega_0$	dimensionless inherent angular frequency
$L$	length, $m$		
$M$	dimensionless mass of vapor plugs	Subscripts	
$m_v$	mass of vapor plugs, $kg$	1	left vapor plug
$P$	dimensionless vapor pressure	2	right vapor plug
$p_v$	vapor pressure, $Pa$	c	condenser
$\wp$	dimensionless parameter defined by Eq. (33)	e	evaporator
$R$	gas constant, $J/kg\ K$	h	heating
$t$	time, $s$	$\ell$	liquid
$T$	temperature, $K$	p	plug
$x_p$	displacement of the liquid slug, $m$	v	vapor
$X_p$	dimensionless displacement of the liquid slug		

equations were solved using an explicit scheme. They concluded that the number of vapor plugs is reduced to the number of heating section no matter how many vapor slugs were initially in the PHP. Zhang and Faghri [10] analyzed a liquid–vapor pulsating flow with thin film evaporation and condensation in a miniature channel with an open end.

Shafii et al.'s [9] results indicated that the performance of the unlooped PHP with two turns are symmetric, i.e., the first and the third vapor plugs have the same pressures and temperatures upon steady oscillation was established. The PHP with two turns can be modeled as two U-shaped channels. The objective of the present study is to analyze the liquid–vapor pulsating flow in a U-shaped miniature tube. The governing equations are first nondimensionalized and the parameters of the system are reduced to several dimensionless numbers. The nondimensional governing equations are then solved numerically and the empirical correlations of amplitude and angular frequency of oscillation will be presented.

## 2. Physical model

A schematic of the U-shaped tube is shown in Fig. 1. A miniature tube with diameter of  $d$  and length  $2L$  is bent into a U-shaped tube with the two ends sealed. The two evaporator sections are near two closed ends, and each of them has a length of  $L_h$ . The condenser section with a length of  $2L_c$  is located at the

bottom of the U-shaped tube. The wall temperatures at the heating and cooling sections are  $T_e$  and  $T_c$ , respectively. A liquid slug with length  $2L_p$  is located at the bottom of the U-shaped tube. The location of the liquid slug is represented by displacement,  $x_p$ , which is zero when the liquid slug is exactly in the middle of the U-shaped miniature tube. When the liquid slug

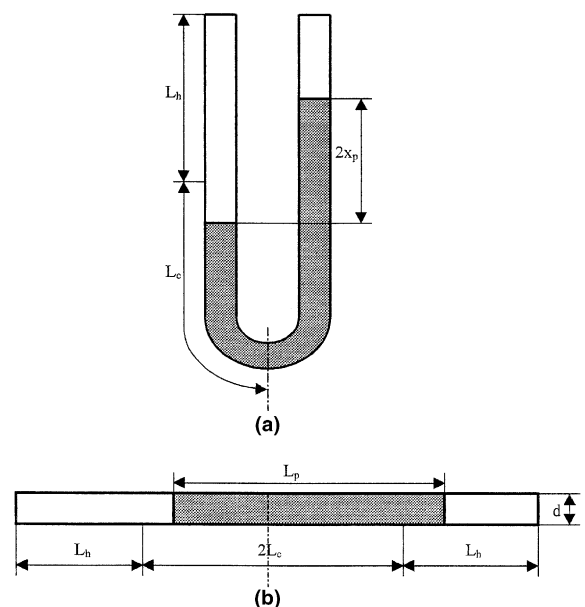


Fig. 1. U-shaped miniature tube.

shifts to the right side, the displacement is positive. When the liquid slug shifts to the left, the displacement is negative.

Suppose the initial value of  $x_{p0}$  is greater than zero, part of the vapor plug in the left side of the heat pipe is in contact with the condenser section, and condensation occurring in the left vapor plug will result in a decrease in the pressure of the left vapor plug,  $p_{v1}$ . On the other hand, part of the right evaporator is in contact with the liquid slug and boiling may occur at the contact area of the right evaporator and liquid slug, which causes increasing vapor pressure of the right vapor plug,  $p_{v2}$ . The liquid plug will be pushed back to the left side due to the pressure difference between the two vapor plugs,  $\Delta p = p_{v1} - p_{v2} < 0$ . When  $x_p$  becomes zero, there is no evaporation or condensation in two vapor plugs, but the liquid slug keeps moving due to its inertia. When part of the liquid slug enters the left evaporator, part of the right vapor plug will be in contact with the condenser. At this point, the boiling in the left vapor plug and condensation in the right plug will change the sign of  $\Delta p$ , and this will result in motion of liquid slug to the right side. The oscillation of the liquid slug can be maintained by alternative boiling and condensation in the two vapor plugs.

### 2.1. Governing equations

The momentum equation for the liquid slug in Fig. 1 can be expressed as

$$A_c L_p \rho_l \frac{d^2 x_p}{dt^2} = (p_{v1} - p_{v2}) A_c - 2 \rho_l g A_c x_p - \pi d L_p \tau_p, \quad (1)$$

where  $A_c = \frac{1}{4} \pi d^2$  is the cross-sectional area of the tube.

Eq. (1) can be rearranged as

$$\frac{d^2 x_p}{dt^2} + \frac{32 v_e}{d^2} \frac{dx_p}{dt} + \frac{2g}{L_p} x_p = \frac{\Delta p}{\rho_l L_p}, \quad (2)$$

where  $v_e$  is the effective kinetic viscosity of the liquid.

The energy equation of the vapor plugs is obtained by applying the first law of thermodynamics to each plug

$$\frac{d(m_{v1} c_v T_{v1})}{dt} = c_p T_{v1} \frac{dm_{v1}}{dt} - p_{v1} \frac{\pi}{4} d^2 \frac{dx_p}{dt}, \quad (3)$$

$$\frac{d(m_{v2} c_v T_{v2})}{dt} = c_p T_{v2} \frac{dm_{v2}}{dt} + p_{v2} \frac{\pi}{4} d^2 \frac{dx_p}{dt}. \quad (4)$$

Eqs. (3) and (4) can be rearranged as

$$m_{v1} c_v \frac{dT_{v1}}{dt} = RT_{v1} \frac{dm_{v1}}{dt} - p_{v1} \frac{\pi}{4} d^2 \frac{dx_p}{dt}, \quad (5)$$

$$m_{v2} c_v \frac{dT_{v2}}{dt} = RT_{v2} \frac{dm_{v2}}{dt} + p_{v2} \frac{\pi}{4} d^2 \frac{dx_p}{dt}. \quad (6)$$

It is assumed that the behavior of vapor plugs in the two evaporators can be modeled using ideal gas law

$$p_{v1} (L_h + x_p) \frac{\pi}{4} d^2 = m_{v1} R_g T_{v1}, \quad (7)$$

$$p_{v2} (L_h - x_p) \frac{\pi}{4} d^2 = m_{v2} R_g T_{v2}. \quad (8)$$

Differentiating Eq. (7) with respect to time gives

$$\begin{aligned} \frac{\pi}{4} d^2 (L_h + x_p) \frac{dp_{v1}}{dt} + p_{v1} \frac{\pi}{4} d^2 \frac{dx_p}{dt} \\ = m_{v1} R \frac{dT_{v1}}{dt} + RT_{v1} \frac{dm_{v1}}{dt} \end{aligned} \quad (9)$$

and substituting Eq. (5) into Eq. (9)

$$RT_{v1} \frac{dm_{v1}}{dt} = \frac{\pi}{4} d^2 \frac{c_v}{c_p} (L_h + x_p) \frac{dp_{v1}}{dt} + p_{v1} \frac{\pi}{4} d^2 \frac{dx_p}{dt}. \quad (10)$$

Substituting Eq. (7) into Eq. (10), a differential equation of  $m_{v1}$  is obtained:

$$\frac{1}{m_{v1}} \frac{dm_{v1}}{dt} = \frac{1}{\gamma} \frac{1}{p_{v1}} \frac{dp_{v1}}{dt} + \frac{1}{L_h + x_p} \frac{dx_p}{dt}, \quad (11)$$

where  $\gamma = c_p/c_v$  is the specific heat ratio of the vapor.

Integrating Eq. (11), a closed form of the mass of the left vapor plug is obtained:

$$m_{v1} = C_1 p_{v1}^{1/\gamma} (L_h + x_p). \quad (12)$$

Substituting Eq. (12) into Eq. (7) yields the temperature of the left vapor plug

$$T_{v1} = \frac{\pi d^2}{4 C_1 R} p_{v1}^{(\gamma-1)/\gamma}. \quad (13)$$

Similarly, the mass and temperature of the right vapor plug can be expressed as

$$m_{v2} = C_2 p_{v2}^{1/\gamma} (L_h - x_p), \quad (14)$$

$$T_{v2} = \frac{\pi d^2}{4 C_2 R} p_{v2}^{(\gamma-1)/\gamma}, \quad (15)$$

where  $C_1$  in Eqs. (12) and (13) and  $C_2$  in Eqs. (14) and (15) are the integration constants. Since the structure of the U-shaped heat pipe is symmetric, these two integration constants are the same, i.e.,  $C_1 = C_2 = C$ .

The masses of the vapor plugs increase due to evaporation and decrease due to condensation

$$\frac{dm_{v1}}{dt} = \begin{cases} -h_c \pi d x_p (T_{v1} - T_c) / h_{fg}, & x_p > 0, \\ -h_c \pi d (L_h + x_p) (T_e - T_{v1}) / h_{fg}, & x_p < 0, \end{cases} \quad (16)$$

$$\frac{dm_{v2}}{dt} = \begin{cases} h_c \pi d (L_h - x_p) (T_e - T_{v2}) / h_{fg}, & x_p > 0, \\ h_c \pi d x_p (T_{v2} - T_c) / h_{fg}, & x_p < 0. \end{cases} \quad (17)$$

## 2.2. Nondimensional governing equations

In order to nondimensionalize the governing equations, a reference state of the U-shaped miniature tube needs to be specified. At this reference state, the pressure and temperature of both vapor plugs are  $p_{v1} = p_{v2} = p_0$ ,  $T_{v1} = T_{v2} = T_0$ . The displacement of liquid plug at reference state is  $x_p = x_{p0}$ . According to Eqs. (13) and (15), the constants  $C_1$  and  $C_2$  are

$$C_1 = C_2 = \frac{\pi d^2}{4RT_0} p_0^{(\gamma-1)/\gamma}. \quad (18)$$

The masses of the two vapor plugs at the reference state are

$$m_{v10} = \frac{\pi d^2}{4RT_0} p_0 (L_h + x_p), \quad (19)$$

$$m_{v20} = \frac{\pi d^2}{4RT_0} p_0 (L_h - x_p). \quad (20)$$

The average mass of two vapor plugs is

$$m_0 = \frac{m_{v10} + m_{v20}}{2} = \frac{\pi d^2}{4RT_0} p_0 L_h. \quad (21)$$

Substituting Eqs. (18) and (21) into Eqs. (12)–(15), one gets

$$\frac{m_{v1}}{m_0} = \left( \frac{p_{v1}}{p_0} \right)^{1/\gamma} \frac{L_h + x_p}{L_h}, \quad (22)$$

$$\frac{T_{v1}}{T_0} = \left( \frac{p_{v1}}{p_0} \right)^{(\gamma-1)/\gamma}, \quad (23)$$

$$\frac{m_{v2}}{m_0} = \left( \frac{p_{v2}}{p_0} \right)^{1/\gamma} \frac{L_h - x_p}{L_h}, \quad (24)$$

$$\frac{T_{v2}}{T_0} = \left( \frac{p_{v2}}{p_0} \right)^{(\gamma-1)/\gamma}. \quad (25)$$

By defining

$$\begin{aligned} \theta_1 &= \frac{T_{v1}}{T_0}, & \theta_2 &= \frac{T_{v2}}{T_0}, & P_1 &= \frac{p_{v1}}{p_0}, \\ P_2 &= \frac{p_{v2}}{p_0}, & M_1 &= \frac{m_{v1}}{m_0}, & M_2 &= \frac{m_{v2}}{m_0}, & X_p &= \frac{x_p}{L_h}, \end{aligned} \quad (26)$$

Eqs. (22)–(25) become

$$M_1 = P_1^{1/\gamma} (1 + X_p), \quad (27)$$

$$\theta_1 = P_1^{(\gamma-1)/\gamma}, \quad (28)$$

$$M_2 = P_2^{1/\gamma} (1 - X_p), \quad (29)$$

$$\theta_2 = P_2^{(\gamma-1)/\gamma}. \quad (30)$$

Introducing the nondimensional variables to Eq. (2) and defining dimensionless time as

$$\tau = \frac{v_e t}{d^2}. \quad (31)$$

Eq. (2) becomes

$$\frac{d^2 X_p}{d\tau^2} + 32 \frac{dX_p}{d\tau} + \omega_0^2 X_p = \wp (P_1 - P_2), \quad (32)$$

where  $\omega_0$  and  $\wp$  are two dimensionless parameters defined as

$$\omega_0^2 = \frac{2gd^4}{L_p v_e^2}, \quad \wp = \frac{p_0 d^4}{\rho_\ell L_p L_h v_e^2}. \quad (33)$$

Substituting Eqs. (26) and (31) into Eqs. (16) and (17), one obtains

$$\frac{dM_1}{d\tau} = \begin{cases} -H_c X_p (\theta_1 - \theta_c), & X_p > 0, \\ -H_e (1 + X_p) (\theta_e - \theta_1), & X_p < 0, \end{cases} \quad (34)$$

$$\frac{dM_2}{d\tau} = \begin{cases} H_e (1 - X_p) (\theta_e - \theta_2), & X_p > 0, \\ H_c X_p (\theta_2 - \theta_c), & X_p < 0, \end{cases} \quad (35)$$

where

$$H_c = \frac{4h_c RT_0^2 d}{p_0 h_{fg} v_e}, \quad H_e = \frac{4h_e RT_0^2 d}{p_0 h_{fg} v_e}, \quad (36)$$

$$\theta_e = \frac{T_e}{T_0}, \quad \theta_c = \frac{T_c}{T_0}.$$

The system is described by six nondimensional parameters defined in Eq. (33) and (36). If the reference temperature is chosen to be the average of  $T_e$  and  $T_c$ , the dimensionless temperature of heating and cooling sections is

$$\theta_e = 1 + \Theta, \quad \theta_c = 1 - \Theta, \quad (37)$$

where

$$\Theta = \frac{T_e - T_c}{T_e + T_c}. \quad (38)$$

At this point, the number of dimensionless parameters that describe the system are further reduced to five.

## 2.3. Initial conditions

The reference state of the U-shaped miniature tube is chosen to be the initial state of the system. The initial conditions of the system are:

$$X_p = X_0, \quad \tau = 0, \quad (39)$$

$$P_1 = P_2 = 1, \quad \tau = 0, \quad (40)$$

$$\theta_1 = \theta_2 = 1, \quad \tau = 0, \quad (41)$$

$$M_1 = 1 + X_0, \quad M_2 = 1 - X_0, \quad \tau = 0. \quad (42)$$

### 3. Numerical solution

The oscillatory flow in a U-shaped miniature tube is described by Eqs. (27)–(30), (32) and (34), (35) with initial conditions specified by Eqs. (39)–(42). The parameters that define the problems are  $\omega_0, \varphi, H_c, H_e, \Theta$  and  $X_0$ .

Note that Eq. (32) is an ordinary differential equation of forced vibration. If the vapor pressure difference between the two vapor plugs is

$$\Delta P = A \cos \omega \tau, \tag{43}$$

the solution of Eq. (32) is

$$X_p = B_0 e^{-16\tau} \cos \left( \sqrt{\omega_0^2 - 16\tau} + \phi_0 \right) + \frac{\varphi A \cos(\omega \tau - \psi)}{\sqrt{(\omega_0^2 - \omega^2)^2 + 1024\omega^2}}, \tag{44}$$

where  $B_0$  and  $\phi_0$  are constants determined by initial conditions of the vibration. The phase difference between  $X_p$  and  $\Delta P$  is

$$\tan \psi = \frac{32\omega}{\omega_0^2 - \omega^2}. \tag{45}$$

The first term of Eq. (44) accounts for the effect of initial conditions of vibration. With increasing time, the energy put into the system by the initial condition is dissipated through damping force and the motion then represents the response of the system to the pressure difference described by Eq. (43). When time is sufficiently long, Eq. (44) becomes

$$X_p = B \cos(\omega \tau - \psi), \tag{46}$$

where

$$B = \frac{\varphi A}{\sqrt{(\omega_0^2 - \omega^2)^2 + 1024\omega^2}}. \tag{47}$$

In reality, the amplitude and angular frequency are unknown a priori and the pressure difference between the two vapor plugs depends on heat transfer in two vapor plugs. The amplitude and angular frequency of pressure oscillation must be obtained by a numerical solution.

The results of each time-step are obtained by solving the dimensionless governing equations using an implicit scheme. The numerical procedure for a particular time step are outlined as follows:

1. Assume  $\theta_1$  and  $\theta_2$ .
2. Solve for  $P_1$  and  $P_2$  from Eqs. (28) and (30).
3. Solve for  $X_p$  from Eq. (32).
4. Calculate the mass of the two vapor plugs,  $M_1$  and  $M_2$ , using Eqs. (34) and (35).
5. Calculate the nondimensional pressure of the two vapor plugs,  $P_1$  and  $P_2$ , from Eqs. (27) and (29).

6. Solve for  $\theta_1$  and  $\theta_2$  from Eqs. (28) and (30).
7. Compare  $\theta_1$  and  $\theta_2$  obtained in step 5 with the assumed values in step 1. If the differences meet a tolerance go to the next step; otherwise, steps 2–5 are repeated until a converged solution is obtained.

The time-step independent solution of the problem can be obtained when time-step is  $\Delta \tau = 10^{-5}$ , which is then used in all numerical simulations.

### 4. Results and discussion

Fig. 2(a) shows the comparison of the liquid slug displacements obtained by the present model and the model of Shafii et al. [9]. The results of Shafii et al.'s model [9] was obtained by using the following parameters:  $L_h = 0.1$  m,  $L_c = 0.1$  m,  $L_p = 0.2$  m,  $d = 3.34$  mm,  $T_c = 123.4$  °C,  $T_e = 20$  °C, and  $h_e = h_c = 200$  W/m<sup>2</sup> K. The present results were obtained by using the corresponding nondimensional parameters:  $\omega_0^2 = 1.2 \times 10^4$ ,  $\varphi = 1.2 \times 10^5$ ,  $\Theta = 0.15$ , and  $H_e = H_c = 3000$ . It can be seen that the results obtained by using the present model agreed very well with Shafii et al.'s model [9]. Consider the unique features of the present model: (1) The U-shaped miniature tube was described by five dimensionless parameters; (2) The closed form solutions of vapor mass and vapor temperatures were obtained; (3) An unconditional stable implicit scheme was employed to solve the problem, the present model represents a significant advancement over the existing models.

Fig. 2(b) shows the effect of dimensionless initial displacement on the oscillatory flow in the U-shaped miniature tube. The initial displacement has significant effect on the first several periods of oscillation. After five periods of oscillation, the amplitudes and angular

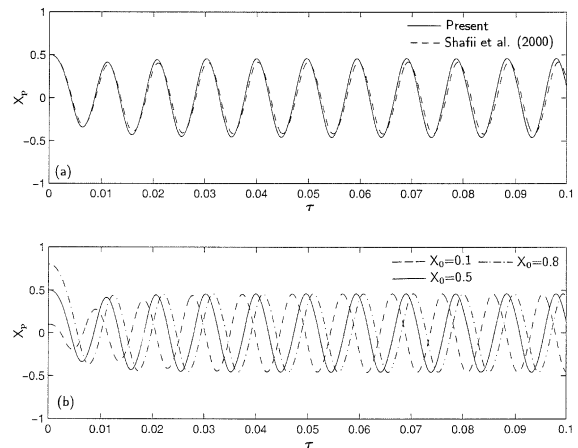


Fig. 2. Oscillation of the liquid slug: (a) comparison with Shafii et al. (2000); (b) effect of initial displacement ( $\omega_0^2 = 1.2 \times 10^4$ ,  $\varphi = 1.2 \times 10^5$ ,  $\Theta = 0.15$ ,  $H_e = H_c = 3000$ ).

frequencies of oscillation for different initial displacements are almost the same. On the other hand, the phase of the oscillation is different for different initial displacements. When the initial displacement is increased, the oscillation of liquid plug is delayed.

Fig. 3 shows the variations of dimensionless temperature, pressure, and mass with time. It is seen that the phase difference between the temperatures in the two vapor plugs is approximately  $\pi$ . The maximum temperature of the vapor plug can exceed the heating wall temperature of miniature tube due to compression of the vapor plug. The difference between the phases of pressure in two vapor plug is also about  $\pi$ . On the other hand, the mass of two vapor plugs vary with same period as the displacement and pressure but it is more like saw tooth wave.

Fig. 4 shows the effect of gravity on the oscillatory flow in the U-shaped miniature tube. It can be seen that the effect of gravity on the oscillation is not significant. The amplitude of the displacement, temperature and pressure of the vapor plugs are slightly increased when gravity is neglected, which qualitatively agrees with Eq. (47). The oscillation phase is advanced when gravity is neglected. The effect of  $\varphi$  on the oscillation in a PHP is shown in Fig. 5. It can be seen that the effect of  $\varphi$  on the amplitude of oscillation is negligible, but the angular frequency of the oscillation is increased by about 40% when  $\varphi$  is doubled.

The effect of  $\Theta$  on the oscillatory flow in the miniature tube is shown in Fig. 6. Fig. 6 shows that the amplitude of  $X_p$  increases with increasing  $\Theta$ . The maximum temperature increases and the minimum temperature decreases with increasing  $\Theta$ . The increase in maximum temperature is larger than the decrease of the minimum temperature which means that the average temperature of the vapor plug increases with increasing  $\Theta$ . As can be

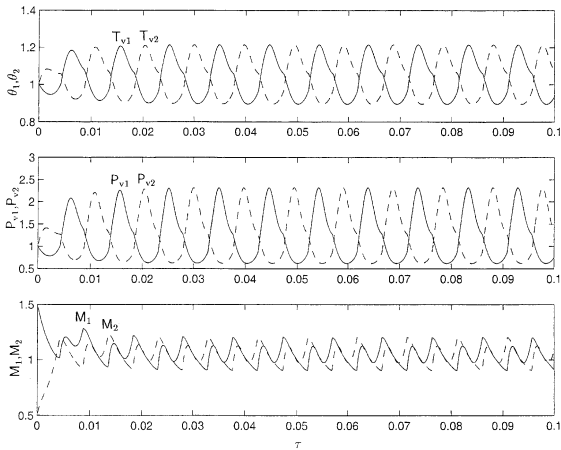


Fig. 3. Dimensionless temperature, pressure and mass of the vapor plugs ( $\omega_0^2 = 1.2 \times 10^4$ ,  $\varphi = 1.2 \times 10^5$ ,  $\Theta = 0.15$ ,  $H_c = H_c = 3000$ ,  $X_0 = 0.5$ ).

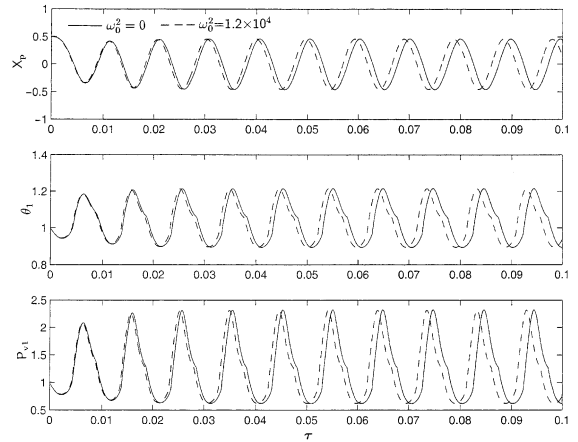


Fig. 4. Effect of gravity on the pulsating flow ( $\varphi = 1.2 \times 10^5$ ,  $\Theta = 0.15$ ,  $H_c = H_c = 3000$ ).

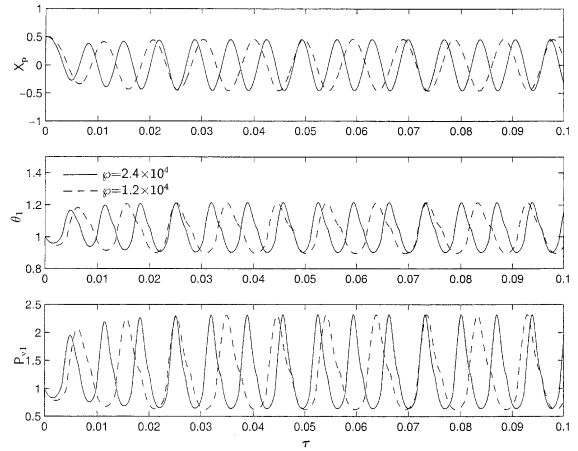


Fig. 5. Effect of  $\varphi$  on the pulsating flow ( $\omega_0^2 = 1.2 \times 10^4$ ,  $\Theta = 0.15$ ,  $H_c = H_c = 3000$ ).

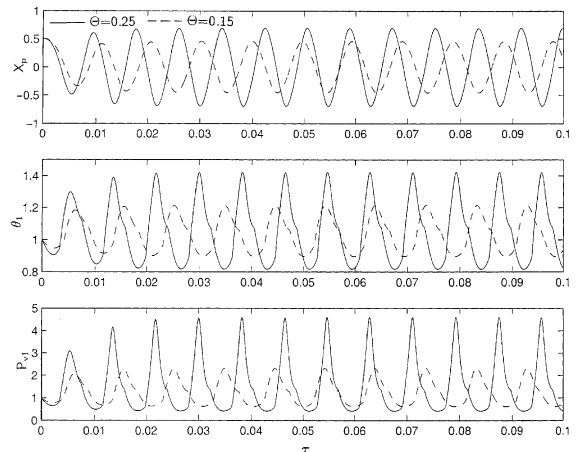


Fig. 6. Effect of  $\Theta$  on the pulsating flow ( $\omega_0^2 = 1.2 \times 10^4$ ,  $\varphi = 1.2 \times 10^5$ ,  $H_c = H_c = 3000$ ).

seen from Fig. 6(c), the average pressure of the vapor plug increases with increasing  $\Theta$  which is very similar to the trend of the temperature. The effect  $H_e$  and  $H_c$  on the oscillatory flow is then investigated. Fig. 7 shows the results for the cases in which the dimensionless heat transfer coefficient at the heating and cooling sections are the same, i.e.  $H_e = H_c = H$ . It can be seen that the amplitude of oscillation slightly increase with increasing heat transfer coefficients. The angular frequency of oscillation is however, decreased with increasing heat transfer coefficients.

The effect of  $\Theta$  on the amplitude of displacement,  $B$ , at different heat transfer coefficients is investigated and the results are partially illustrated in Fig. 8. It can be seen that the amplitude is a monotonic function of dimensionless temperature difference, and the slope of the  $B-\Theta$  curve decreases with increasing dimensionless heat transfer coefficient. The amplitude of the displacement can be correlated as function of  $\Theta$  and  $H$

$$B = \sum_{i=1}^3 \sum_{j=1}^4 b_{ij} (H \times 10^{-3} - 3)^{j-1} (\Theta - 0.175)^{i-1},$$

$$1000 < H < 5000, \quad 0.05 < \Theta < 0.25, \quad (48)$$

where

$$[b_{ij}] = \begin{bmatrix} 0.52801 & 0.013934 & -0.81339 \times 10^{-2} \\ 2.60870 & -0.13483 & -0.22955 \times 10^{-1} \\ -5.0681 & -0.16342 & 0.62381 \times 10^{-2} \\ 0.31055 \times 10^{-2} \\ 0.68034 \times 10^{-2} \\ -0.34886 \times 10^{-1} \end{bmatrix} \quad (49)$$

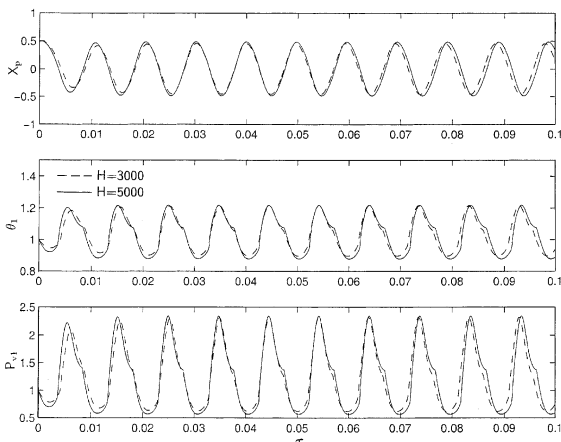


Fig. 7. Effect of dimensionless heat transfer coefficient on the pulsating flow ( $\omega_0^2 = 1.2 \times 10^4$ ,  $\varphi = 1.2 \times 10^5$ ,  $\Theta = 0.15$ ).

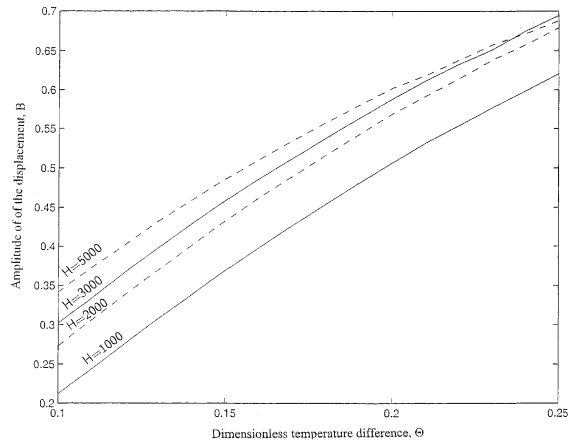


Fig. 8. Amplitude of of the displacement ( $\omega_0^2 = 1.2 \times 10^4$ ,  $\varphi = 1.2 \times 10^5$ ).

and the maximum error that obtained by Eq. (48) is less than 1%.

Similarly, the effect of  $\Theta$  on the angular frequency,  $\omega$ , at different heat transfer coefficients is investigated and the results are partially illustrated in Fig. 9. The angular frequency is a monotonic function of dimensionless temperature difference and slope of the  $\omega-\Theta$  curve increases with increasing dimensionless heat transfer coefficients. The angular frequency of oscillation can be correlated as

$$\omega = \sum_{i=1}^3 \sum_{j=1}^4 \varphi_{ij} (H \times 10^{-3} - 3)^{j-1} (\Theta - 0.175)^{i-1},$$

$$1000 < H < 5000, \quad 0.05 < \Theta < 0.25, \quad (50)$$

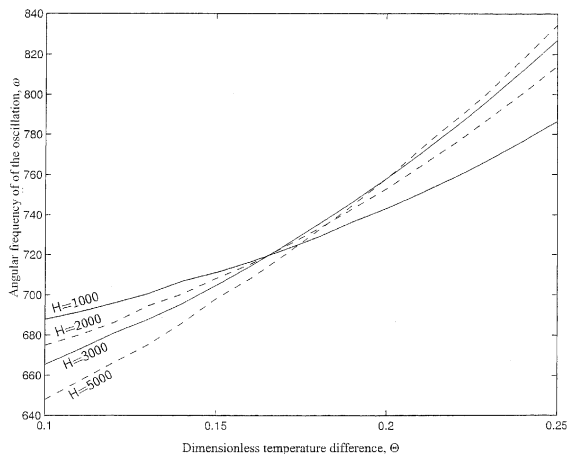


Fig. 9. Angular frequency of of the oscillation ( $\omega_0^2 = 1.2 \times 10^4$ ,  $\varphi = 1.2 \times 10^5$ ).

where

$$[\varphi_{ij}] = \begin{bmatrix} 729.72 & 0.13251 & -0.96554 & -0.024579 \\ 1074.1 & 114.44 & -31.324 & 8.0407 \\ 3006.2 & -71.904 & -168.07 & 63.906 \end{bmatrix} \quad (51)$$

and the maximum errors that obtained by Eq. (50) is less than 0.5%.

## 5. Conclusion

Oscillatory flows in a U-shaped miniature tube are investigated in the present study. The governing equations of the oscillatory flow were nondimensionalized and the nondimensional parameters that describe the system were reduced to five. The results show that the initial displacement of the liquid slug has an insignificant effect on the amplitude and angular frequency of the oscillation. The effect of gravity on the oscillatory flow is also insignificant. The effect of dimensionless temperature difference and heat transfer coefficient on the amplitude and angular frequency were investigated. The correlations of amplitude and angular frequency of oscillation were obtained and the maximum errors were within 1% and 0.5%, respectively.

## Acknowledgements

Funding for this work was provided by NASA Grant NAG3-1870 and NSF Grant CTS 9706706.

## References

- [1] H. Akachi, Looped capillary heat pipe, Japanese Patent no. Hei6-97147, 1994.
- [2] H. Akachi, F. Polasek, P. Stulc, Pulsating heat pipes, in: Proceedings of the 5th International Heat Pipe Symposium, Melbourne, Australia, 1996, pp. 208–217.
- [3] K. Gi, S. Maezawa, Y. Kojima, N. Yamazaki, CPU cooling of notebook PC by oscillating heat pipe, in: Proceedings of the 11th International Heat Pipe Conference, Tokyo, Japan, 1999, pp. 166–169.
- [4] Y. Miyazaki, H. Akachi, Heat transfer characteristics of looped capillary heat pipe, in: Proceedings of the 5th International Heat Pipe Symposium, Melbourne, Australia, 1996, pp. 378–383.
- [5] Y. Miyazaki, M. Arikawa, Oscillatory flow in the oscillating heat pipe, in: Proceedings of the 11th International Heat Pipe Conference, Tokyo, Japan, 1999, pp. 131–136.
- [6] Y. Miyazaki, H. Akachi, Self excited oscillation of slug flow in a micro channel, in: Proceedings of the 3rd International Conference on Multiphase Flow, Lyon, France, 1998.
- [7] H.W. Lee, S.H. Jung, H.J. Kim, J.S. Kim, Flow visualization of oscillating capillary tube heat pipe, in: Proceedings of the 11th International Heat Pipe Conference, Tokyo, Japan, 1999, pp. 131–136.
- [8] M. Hosoda, S. Nishio, R. Shirakashi, Meandering closed-loop heat-transport tube (propagation phenomena of vapor plug), in: Proceedings of the 5th ASME/JSME Joint Thermal Engineering Conference, San Diego, CA, 1999.
- [9] B.M. Shafii, A. Faghri, Y. Zhang, Thermal modeling of unlooped and looped pulsating heat pipes, ASME J. Heat Transfer 123 (6) (2001) 1159–1172.
- [10] Y. Zhang, A. Faghri, Heat transfer in a pulsating heat pipe with open end, Int. J. Heat Mass Transfer 45 (4) (2002) 755–764.